Chinese J. of Chem. Eng., **7** (2) 116−125 (1999)

Heat Transfer Between Immersed Horizontal Tubes and Aerated Vibrated Fluidized Beds*

Ye Shichao(叶世超), Li Chuanna(李川娜) and Cheng Kuangmin(陈匡民)**
Department of Chemical Engineering, Sichuan Union University, Chengdu 610065, China

Abstract Heat transfer coefficients between an immersed horizontal tube and an aerated vibrated fluidized bed are measured. There is a maximum value in the h-Γ experimental curve. The heat transfer coefficient increases with decreases in particle diameter in the fully fluidized region. The particle density has less effect on the heat transfer coefficients. High amplitude and low frequency, or low amplitude and high frequency are favorable to heat transfer. Exceedingly high gas velocity is unfavorable to the surface-bed heat transfer. A model based on the 'pocket' theory was proposed for predicting the surface-to-bed heat transfer coefficients in fully fluidized region. The predictions from the model were compared with observed data. The reasonable fit suggests the adequacy of the model.

Keywords vibration heat transfer, vibration fluidization, heat transfer, vibration, fluidization

1 INTRODUCTION

Tubes are horizontally immersed in the granular layer of a fluidized bed, and the two ends of the tubes are rigidly fixed in wall of the bed. When the bed with the horizontal tubes is vibrated in the vertical direction, the particles will be fluidized under the dual actions of gas flow and vibration. At this time, the heat transfer rates between the surface of tubes and the layer of the beds can be greatly increased for rapidly putting heat into or removing heat from the bed to meet the need of various processes for heat. For example, a sort of aerated vibrated fluidized dryer has been designed based on this principle. Advantages of the new dryer over conventional vibrated or non-vibrated fluidized dryers are not only in its small equipment size and low energy dissipation, but also in its excellent dispersion action on the lump material with high moisture content. It can be expected that there be a very good application prospect in process industries[1]. But , there are very few studies on heat transfer between vibrated fluidized beds and vibrated horizontal tubes, and little published information is available for design. Up to now, mathematical models concerned with this phenomenon are not available and the mechanism is not well known. So, it is very necessary for us to gain further insight in the phenomenon.

The high rate of heat transfer between fluidized beds and immersed surfaces in attributed to the intensive displacement of particles on the surface[2]. When there is no vibration, *i.e.*, heat transfer between fluidized bed and stationary surface, this displacement results from only gas bubbles[3]. But, when there is vibration, *i.e.*, heat transfer between the vibrated fluidized bed and the furface immersed in the bed, the displacement of particles on surfaces is attributed to the action of vibration on the layer of particles. The intensive vibration of the surface is taken to be responsible for speeding the displacement of particle on the surface and increasing the transfer of heat.

Malhotra and Mujumdar focused on the heat transfer between aerated vibrated fluidized bed

Received 1998-01-06, accepted 1998-11-10.
* Supported by the National Natural Science Foundation of China(No.29576253).
** To whom correspondence should be addressed.

and immersed vibrated horizontal cylinder[4,5]. They noticed that, at the up and down surfaces of the cylinder, the particles are thrown off and then fell down contacting with surface because of vibrating of the cylinder and this forms alternative crescent-like gaps. The heat transfer rate was viewed as the joint result of particle convection and gas convection within the gaps. An equation was proposed to predict heat transfer coefficients by the width of the gap. Eccles and Mujumdar proposed a concept of resonance bed for fine particles[6,7]. For a given u_f/u_{mf} and amplitude, the height of beds reaches the maximum value and the maximum heat transfer coefficient is obtained when the frequency f rise close to the resonance frequency f_r. The dramatically increase of heat transfer coefficients in the vicinity of f_r was attributed to the high-speed moving and the perfectly mixing of particles. A semiempirical correlation is developed to calculate heat transfer coefficients by means of the dampening factor of the system. Because such parameters as the dampening factor and the extent of gap coverage are unknown, these methods of calculating heat transfer coefficient are not convenient for engineering calculation.

2 EXPERIMENT APPARATUS AND PROCEDURE

A schematic sketch of the experimental set-up is illustrated in Fig. 1. A two-dimensional fluidized bed, cross section 240 mm×80 mm, was designed and fabricated for operating at room temperature. The bed was made from Plexiglass plate to permit visual observations of the fluidization conditions.

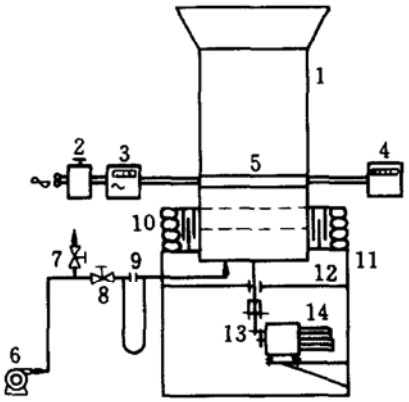

Figure 1 Schematic sketch of experimental equipment
1—fluidized bed; 2—voltage regulator; 3—wattmeter; 4—digital thermometer; 5—tube; 6—blower; 7—bypass valve; 8—control valve; 9—orifice meter; 10—springs; 11—vibrating platfrom; 12—stright-line bearings; 13—eccentric mechanism; 14—variable speed motor

The distributor consisted of a perforated plate and a stainless steel screen on the plate. A porous plate was assembled at the position of 30 mm beneath the distributor to gain a more homogeneous distribution of gas flow.

The bed body, supported on four springs, was vibrated in the vertical direction by means of an eccentric mechanism. The amplitude was adjusted by changing the eccentricity of the system and the frequency was controlled by means of the variable speed motor. Five straight-line movement bearings were mounted on the bed body to prevent it from swinging horizontally.

The tube, 25 mm in diameter and 60 mm in length, was made from copper cylinder imbedded with a small cylindrical heater and extended on both poles with Teflon ends of the same diameter to prevent heat from axially flowing. The tube was rigidly and horizontally assembled in the central mid-plane of the bed, its axial center being located 60 mm above the distributor. Four copper-constantan thermocouples were welded at the surface around periphery of the tube to measure the surface temperatures, one of the thermocouples was mounted 3 mm from one end to measure the axial variation of temperatures, and the others were placed on the central surface at 0°, 90°, 180° to permit the measurement of the average surface temperatures.

The temperatures of the bed and those of the tube surface were monitored with an electronic digital thermometer. The power inputted to the heater was adjusted by a voltage regulator and measured with a single-phase wattmeter. The gas velocity was regulated by an orifice meter.

Various materials, with different size, density and shape, were used as model particles, and their physical properties are listed in Table 1. Table 2 shows the rage of the parameters used in this study.

Heat transfer coefficients were measured under steady state. The bed was vibrated under given air velocity and amplitude and frequency, and the power into heater was switched on. The experiment was started and continued until the temperature of the tube surface reached a constant value. The surface-bed heat transfer coefficient is determined according to

$$h = \frac{P}{A_W(T_w - T_b)} \tag{1}$$

Table 1 Physical properties of particles

Particle	Size mm	Density $kg \cdot m^{-3}$	Bulk density $kg \cdot m^{-3}$	Voidage	Mini-fluid velocity $m \cdot s^{-1}$
rice	3	1373	810	0.41	0.775
foxtail millet	1.42	1298	758	0.416	0.132
sugar	0.99	1509	812	0.462	0.33
sand 1	1.3	2662	1494	0.43	0.74
sand 2	0.85	2498	1440	0.43	0.50
sand 3	0.6	2380	1420	0.416	0.47
arenaceous quartz	1.3	2500	1344	0.462	0.96
glass ballotini	0.3	2485	1420	0.427	0.132

Table 2 Range of operating parameters

Variables	Minimum	Maximum
vibration acceleration	0	4.0
vibration amplitude, mm	0	4.0
vibration frequency, Hz	0	32
gas velocity (u_f/u_{mf})	0	1.2
bed height, mm	100	120
particle size, mm	0.3	3.0
particle density, $kg \cdot m^{-3}$	780	2500
bulk density, $kg \cdot m^{-3}$	520	1450
particle sphericity	0.62	1

where P is the power inputted to the heater, T_w and T_b are the temperature of the tube surface and the temperature of the bed, respectively.

The vibration acceleration in Table 2 is dimensionless. It is defined as

$$\Gamma = A\omega^2/g \tag{2}$$

3 EXPERIMENTAL RESULTS

3.1 Effect of vibration parameters on heat transfer coefficients

variations of heat transfer coefficients with vibration accelerations are shown in Fig. 2 for sand of 0.6 mm in diameter. It is noticed that there is a maximum value in each curve and the vibration

acceleration corresponding to the maximum value decreases with increases in air velocity. This can be attributed to the joint action of the increasing rate of particle displacement on the tube surface and the decrease of contact time of the material layer with the surface when the vibration acceleration increases. This result is consistent with the findings of Malhotra and Mujumdar[5].

Fig. 3 shows the effect of vibration amplitudes on heat transfer coefficients for sand of 0.6 mm in diameter when $u_f/u_{mf} = 0.6$. It can be seen that, under aerated conditions, the amplitude has less influence on heat transfer coefficient. Nevertheless, from Fig. 4 showing the influence of frequencies on heat transfer coefficients, it can be seen that high amplitude and low frequency, or low amplitude and high frequency are favorable to heat transfer.

3.2 Effect of gas velocity on heat transfer coefficients

Fig. 5 shows the variation of heat transfer coefficients with gas velocities. These curves fall into two classes: those of $\Gamma < 1.0$ and those of $\Gamma > 1.0$. The former represent heat transfer for packed beds within the range of lower velocity, and only when the velocity is close to u_{fm} the curves go up rapidly. The latter shows heat transfer for fluidized beds. Because the bed has been fluidized by vibration, the heat transfer coefficients will decline when aerated.

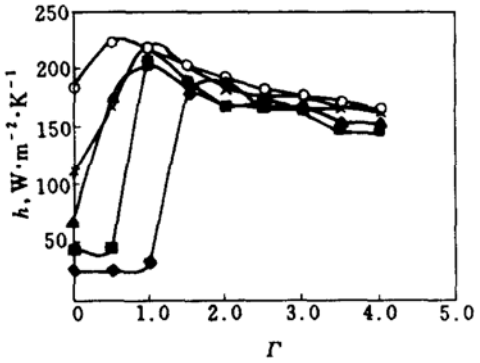

Figure 2 Effect of vibration acceleration on heat transfer coefficients for sand ($d_p = 0.6$ mm)
u_f/u_{mf}: ◆ 0; ■ 0.3; ▲ 0.6; × 0.9; ○ 1.2

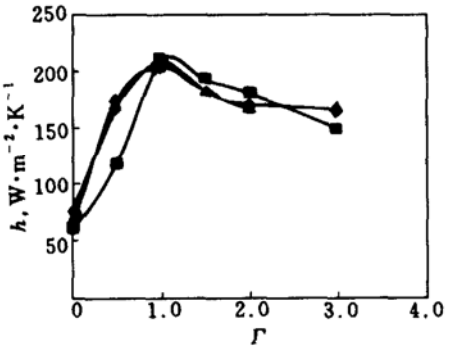

Figure 3 Effect of amplitude on heat transfer coefficient for sand ($u_f/u_{mf} = 0.6$)
A, mm: ◆ 1.0; ■ 2.5; ▲ 4.25

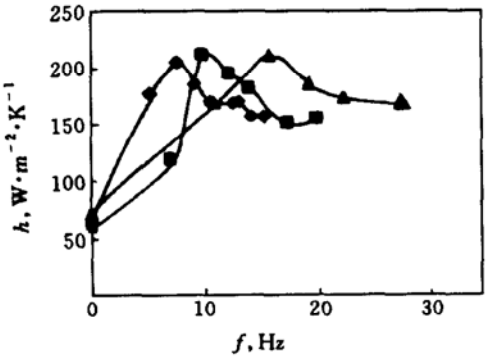

Figure 4 Effect of frequency on heat transfer coefficient for sand ($u_f/u_{mf} = 0.6$)
A, mm: ◆ 4.25; ■ 2.5; ▲ 1.0

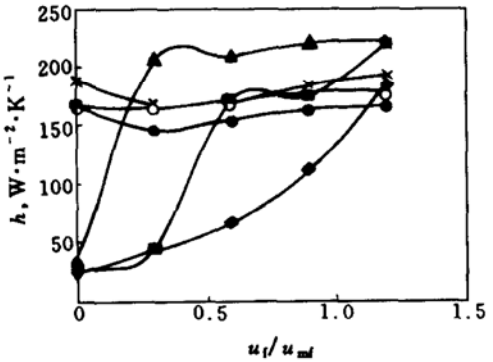

Figure 5 Effect of velocity on heat transfer coefficient for sand ($d_p = 0.6$ mm, $A = 4.25$ mm)
Γ: ◆ 0; ■ 0.5; ▲ 1.0; × 2.0; ○ 3.0; ● 4.0

3.3 Effect of size and density of particles on heat transfer coefficients

The effect of particle size on heat transfer coefficients is shown in Fig. 6, for sand of $d_p = 0.6$, 0.85 and 1.3 mm. The coefficients increase with decreases in particle diameter in the fully fluidized region. This is because smaller particles can achieve more intimate contact with the tube surface and there is less contact thermal resistance at the surface. But, under the same u_f/u_{mf}, larger particles have higher operating velocity, so the convection of gas flow is stronger. This is taken to be responsible for higher coefficients of larger particles in the section of packed bed.

The density of particles has less effect on heat transfer coefficients. This can be seen from Fig. 7. Although the density of sand ($d_p = 1.3$ mm) is approximately twice as high as that of foxtail millet ($d_p = 1.43$ mm), heat transfer coefficients for the sand and the foxtail millet are almost the same in the whole range of vibration acceleration. This is consistent with the conclusion from non-vibrated fluidized beds[8].

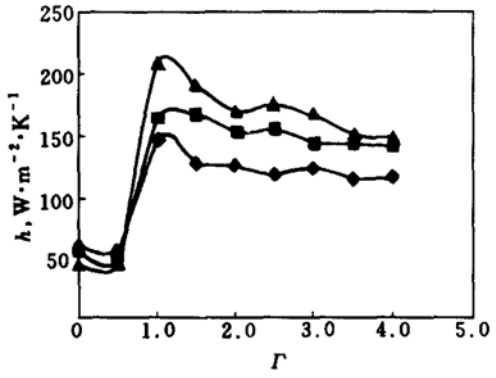

Figure 6 Effect of particle size on heat transfer coefficient for sand
d_p, mm: ◆ 1.3; ■ 0.85; ▲ 0.6

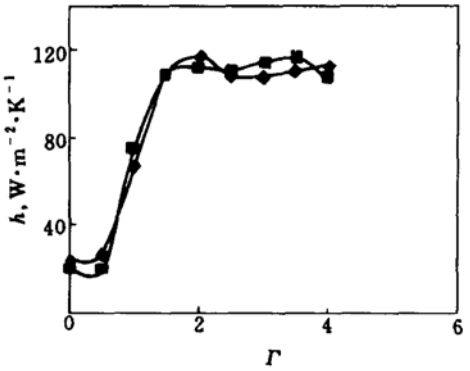

Figure 7 Effect of particle density on heat transfer coefficient for $u_f/u_{mf} = 0$
◆ sand, $d_p = 1.3$ mm; ■ foxtail millet

4 MODEL FOR HEAT TRANSFER

The rate of heat transfer between an immersed tube and a fluidized bed of particles is controlled by dynamics of the bed. There are alternating gas gaps around the horizontal tube as noted by Mujumdar *et al.*[4,6] Moreover, in our experiment, it has been observed that there is a negative pressure region around the tube accompanied by the gap. The pressure has an important influence on movement of particles in the bed especially in the region adjacent to the tube surface.

For different ranges of gas velocity, there are two patterns of bed dynamics. At lower velocities ($u_f/u_{mf} < 0.5$), the negative pressure draws the particles from the upper part of bed to the tube wall, and pushes the particles into the lower part of bed. The particles in the lower part return to the upper part of the bed along the two side sections of the bed and form circulation movement of particles in the whole bed (as shown in Fig. 8). The locus lines of moving particles can be observed clearly in our tracer experiments. At high gas velocities. the negative pressure draws the particles from the lower part of the bed to the tube wall and then presses them into the upper part. Nevertheless, because of the strong action of gas velocity on particles, the circulation movement of particles is very weak.

No matter what pattern of bed dynamics mentioned above, it is reasonable to assume that the residence time of particles on the surface of tube is random and the opportunity of particles

swept onto the surface is also random. Consequently, we can model the phenomenon of heat transfer by a method similar to the 'pocket' theory developed by Mickley[9] and Gelperin[8] for heat transfer between a non-vibrated fluidized bed and an immersed surface.

Consider a pocket of particles at temperature T_b swept into contact with a surface of temperature T_w. Unsteady-state conduction will commence on contact. And then the heated packet of particles is replaced by a new and cold packet of particles from the core portion of beds. If the average residence time of these pockets is t_m, then the mean heat transfer coefficient can be given by

$$h = \frac{1}{R_a} = \frac{q}{T_w - T_b} = \sqrt{\frac{k_{ea} c_s \rho_b}{\pi t_m}} \tag{3}$$

where R_a is the thermal resistance of the particle pockets in the emulsion phase, and k_{ea} and ρ_b are the effective thermal conductivity and density of the pockets, respectively. k_{ea} is predicted in teams of the method recommended by Gelperin[8]. The voidage fraction of the vibrating bed can be predicted approximately by the following equation

$$\varepsilon = \varepsilon_{mf}\left(1 + 5.48\frac{A}{L}\right)\left[1 + \left(\frac{u_f}{u_{mf}}\right)^{0.25}\right] \tag{4}$$

The mean value of contact time of pockets with the tube can be calculated as follows: as shown in Fig. 9, a pocket of particles moves from the highest point of tube wall to the lowest point because of the impetus of the vibrating tube. The tube has a vertical vibration velocity

$$u = 4Af \tag{5}$$

Then the local velocity of the particle pocket along the periphery of the tube wall is

$$u' = u\sin\theta \tag{6}$$

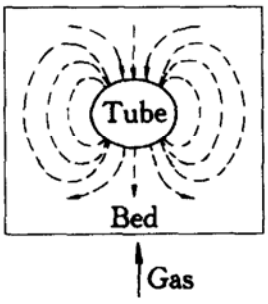

Figure 8 Moving patterns of particles around a tube

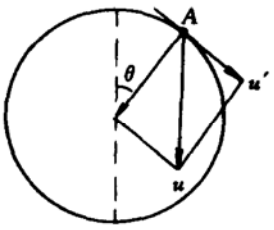

Figure 9 Motion of a particle on tube wall

Since there are gas gaps in the up and down surfaces of tube wall, the rate of heat transfer is so small that it can be neglected. So, it is reasonable to assume that the transfer of heat occurs only at the side-surface of the tube. Hypothesize the section of heat transfer covers half of the tube surface, then the average velocity of the pocket along the periphery of the tube within the

side-surface is expressed by

$$u_{\mathrm{m}} = \frac{1}{\pi/2}\int_{\frac{\pi}{4}}^{\frac{3\pi}{4}} u\sin\theta \mathrm{d}\theta = \frac{8\sqrt{2}}{\pi}Af \tag{7}$$

The residence time of the particle pocket on the side-surface is

$$t_{\mathrm{m}} = \frac{\pi d_{\mathrm{t}}/4}{u_{\mathrm{m}}} = \frac{\pi^2 d_{\mathrm{t}}}{32\sqrt{2}Af} \tag{8}$$

Substituting Eq. (8) into Eq. (3) we obtain

$$R_{\mathrm{a}} = \sqrt{\frac{\pi^3 d_{\mathrm{t}}}{32\sqrt{2}Afk_{\mathrm{ea}}c_{\mathrm{s}}\rho_{\mathrm{b}}}} \tag{9}$$

In addition, Gelperin[8] assumes that, in the non-vibrated fluidized bed, there is an additional contact resistance R_{w} at the surface

$$R_{\mathrm{w}} = \frac{\delta_{\mathrm{w}}}{k_{\mathrm{ew}}} \tag{10}$$

where δ_{w} is the extent of the zone adjacent to the wall, which is of the order of magnitude of the particle radius, $d_{\mathrm{p}}/2$. Under the condition of vibration, to reflect the effect of vibration on the resistance, we assume that R_{w} is expressed approximately by

$$R_{\mathrm{w}} = m\left(\frac{f}{f_{\mathrm{opt}}}\right)^n \frac{d_{\mathrm{p}}}{k_{\mathrm{ew}}} \tag{11}$$

where m and n are parameters determined by experiments. Contact resistance R_{w} is in series with the thermal resistance R_{a} of particle pocket itself and forms the total resistance of heat transfer. Under the condition of T_{w} = constant, Gelpirin has derived a subsequent equation[8]

$$h = \frac{1}{R_{\mathrm{w}} + 0.5R_{\mathrm{a}}} \tag{12}$$

From Eqs. (9), (11) and (12), we get

$$h = \frac{1}{m\left(\frac{f}{f_{\mathrm{opt}}}\right)^n \frac{d_{\mathrm{p}}}{k_{\mathrm{ew}}} + 0.5\sqrt{\frac{\pi^3 d_{\mathrm{t}}}{32\sqrt{2}Afk_{\mathrm{ea}}c_{\mathrm{s}}\rho_{\mathrm{b}}}}} \tag{13}$$

The parameters m and n are determined as follows: if $f = f_{\mathrm{opt}}$, then $f/f_{\mathrm{opt}} = 1$ and $h = h_{\max}$, the value of m can be computed through the point (f_{opt}, $h_{\max}$).

$$m = \left(\frac{1}{h_{\max}} - 0.5\sqrt{\frac{\pi^3 d_{\mathrm{t}}}{32\sqrt{2}Af_{\mathrm{opt}}k_{\mathrm{ea}}c_{\mathrm{s}}\rho_{\mathrm{b}}}}\right) \Big/ \frac{d_{\mathrm{p}}}{k_{\mathrm{ew}}} \tag{14}$$

Having determined the value of m, n can be calculated by the following empirical correlation

$$n = 3.522\times 10^{-3} m^{-0.684}\left(\frac{u_{\mathrm{f}}}{u_{\mathrm{mf}}}\right)^{-0.832}(Ar^{1/3}d_{\mathrm{p}}^3)^{-0.184} \tag{15}$$

By fitting 56 experimental data points of (h_{max}, Γ_{opt}) for 8 materials, we obtain

$$\frac{h_{max}}{\sqrt{0.785(4Af_{opt})k_{ea}c_s\rho_b}} = 20Ar^{-0.208}\Gamma_{opt}^{-0.08}\left(\frac{u_f}{u_{mf}}\right)^{0.324} \tag{16}$$

$$\sqrt{\Gamma_{opt}} = 0.994Ar^{-0.013}\left(\frac{u_f}{u_{mf}}\right)^{-0.26} \tag{17}$$

Eqs. (16) and (17) can represent about 95% of the observed data (h_{max}, Γ_{opt}) within ±20% deviation. From Γ_{opt} we can get f_{opt}

$$f_{opt} = \frac{1}{2\pi}\sqrt{\frac{g\Gamma_{opt}}{A}} \tag{18}$$

Eq. (13) can be used in the range of $\Gamma \geqslant \Gamma_{opt}$ with good accuracy.

5 ANALYSIS AND ASSESSMENT FOR THE EQUATIONS

With the procedure adopted for determining m, the h-Γ curve passes through a point with coordinates (h_{max}, Γ_{opt}). Moreover, the configuration of the curve is adjusted by means of the value of n. The empirical parameter m and n correct the errors associated with assumptions of model, and to certain extent smooth the inaccuracies that result from assumptions used in deriving the calculation equation. It can be expected that the equations have a small deviation in the rage of $\Gamma \geqslant \Gamma_{opt}$. The results of calculation by the equation are in good agreement with the experimental data. Some examples are given in Table 3, Fig. 10 and Fig. 11. It should be explained that Γ adopted in engineering is usually higher than Γ_{opt} needed for transfer of heat. This because the role of vibration is chiefly in dispersion of lump materials.

Although the calculation procedure is relative complex, it should be noticed that the heat transfer coefficient can be calculated only through the technological operation parameters and the physical properties of the system, not through such unknown parameters as c_x, the damping factor[7], and θ, the extent of gap coverage[5]. This is convenient to the engineering calculation.

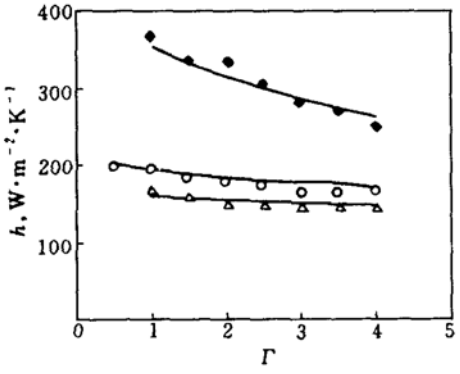

Figure 10 Comparison of experimental data with the correlation
——predicted curve; △ ○ ◆ measured data
△ rice, $u_f/u_{mf} = 0.9$, $A = 4.25$ mm;
○ sand, $d_p = 0.85$ mm, $u_f/u_{mf} = 1.2$, $A = 1.0$ mm;
◆ glass ballotini, $u_f/u_{mf} = 1.2$, $A = 4.25$ mm

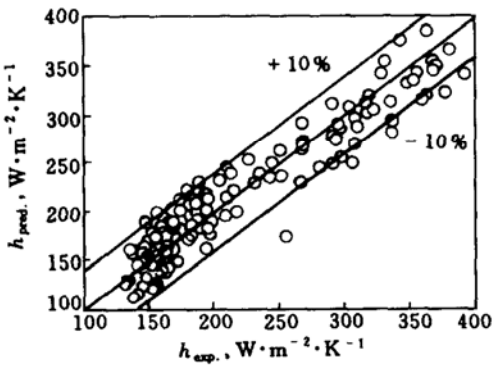

Figure 11 Comparison between experimental and predicted results

Table 3 Experimental and predicted heat transfer coefficients

System	Γ	h, W·m^{-2}·K^{-1} (experimental)	h, W·m^{-2}·K^{-1} (predicted)	Error %
glass bead, $d_p = 0.3$ mm,	1.0	368	354	3.69
$A = 4.5$ mm and $u_f/u_{mf} = 1.2$	1.25	342	343	−0.74
	1.5	336	332	1.28
	2.0	334	313	6.30
	3.0	280	284	−1.48
	4.0	250	263	−5.14
sand, $d_p = 0.85$ mm,	0.5	199	202	−1.48
$A = 1.0$ mm and $u_f/u_{mf} = 1.2$	1.0	198	194	1.87
	1.5	194	188	2.87
	2.0	187	184	1.69
	3.0	175	177	1.02
	4.0	165	171	3.93
rice, $d_p = 3.0$ mm,	1.0	167	160	3.91
$A = 4.25$ mm, $u_f/u_{mf} = 0.9$	1.5	158	157	0.61
	2.0	148	154	−4.44
	2.5	146	152	−4.49
	3.0	145	151	−4.04
	3.5	144	149	−3.76
	4.4	143	148	−3.60

6 CONCLUSIONS

Heat transfer coefficients between an immersed horizontal tube and a vibrated aerated fluidized bed were measured and model equations for predicting surface-to-bed heat transfer coefficients were proposed.

(1) There is a maximum value of heat transfer coefficient in each of the h-Γ experimental curve and the vibration acceleration corresponding to the maximum value decreases with increases in air velocity. The coefficient increases with decreases in particle diameter in the fully fluidized region. The density of particles has less effect on the heat transfer coefficient. High amplitude and low frequency, or low amplitude and high frequency are favorable to heat transfer. Exceedingly high gas velocity is unfavorable to the surface-bed heat transfer.

(2) Heat transfer coefficients are represented with two thermal resistance in series: the resistance of emulsion phase R_a which is developed from the well-known 'pocket' theory of heat transfer between a non-vibrated fluidized bed and an immersed surface, and the contact resistance of particle pocket with surface R_w which is determined from experiment. The expressions for heat transfer coefficients can be give with Eq. (13) in the range of $\Gamma \geqslant \Gamma_{opt}$ with good accuracy.

NOMENCLATURE

A amplitude of vibration, m

A_w surface area of tube, m^2

Ar Archimedes number $[= d_p^3 \rho_f (\rho_s - \rho_f) g/\mu_f^2]$

c_s specific heat capacity of solid particles, W·kg^{-1}·K^{-1}

d_t tube diameter, m

d_p size of particle, m

f	frequency of vibration, Hz
f_{opt}	optimum frequency, Hz
g	gravity acceleration, $m \cdot s^{-2}$
h	heat transfer coefficient, $W \cdot m^{-2} \cdot K^{-1}$
h_{max}	maximum value of h, $W \cdot m^{-2} \cdot K^{-1}$
k_{ea}	effective conductivity of emulsion phase, $W \cdot m^{-1} \cdot K^{-1}$
k_{ew}	effective conductivity of particle pocket on tube surface, $W \cdot m^{-1} \cdot K^{-1}$
L	stationary height of beds, m
m, n	model parameter
q	rate of heat transfer, $W \cdot m^{-2} \cdot K^{-1}$
R_a	thermal resistance of emulsion, $m^2 \cdot K \cdot W^{-1}$
R_w	contact thermal resistance of particle pocket, $m^2 \cdot K \cdot W^{-1}$
T_b	temperature of beds, K
T_w	temperature of tube wall, K
t_m	average residence time of particles on surface, s
u_f	operating gas velocity, $m \cdot s^{-1}$
u_{mf}	minimum fluidizing velocity, $m \cdot s^{-1}$
Γ	vibration acceleration ($= A\omega^2/g$)
Γ_{opt}	value of Γ at h_{max}
δ_w	thickness of contact resistance, m
ε	voidage fraction
ε_{mf}	voidage fraction at u_{mf}
θ	extent of gap coverage, (°)
ρ_b	bulk density of packed beds, $kg \cdot m^{-3}$
ω	angular frequency, s^{-1}

REFERENCES

1 Ye, Sh. Ch., Proceeding of the National Drying Academic Conference, Beijing, 41—45 (1996).
2 Kunii, D., Levenspiel, O., Fluidization Engineering, John Wiley & Sons Inc., New York, 265—300 (1969).
3 Davidson, J. F., Harrison, D., Fluidization, Academic Press, London and New York, 403—446 (1971).
4 Malhotra, K., Mujumdar, A. S., *Can. J. Chem. Eng.*, **63** (1), 22—28 (1985).
5 Malhotra, K., Mujumdar, A. S., *Ind. Eng. Chem Res.*, **26** (10), 1983—1992 (1987).
6 Eccles, E. R. A., Mujumdar, A. S., *Drying Technology*, **10** (1), 139—164 (1992).
7 Eccles, E. R. A., Mujumdar, A. S., *Drying Technology*, **10** (1), 165—187 (1992).
8 Gelperin, N. I., Einstein, V. G., *Khim. Prom.*, **9** (6), 418 (1966).
9 Mickley, H. S., Fairbanks, D. F., *AIChE J.*, **1** (1), 374 (1955).